An Acad Bras Cienc (2025) 97(Suppl. 1): e20250756 DOI 10.1590/0001-3765202520250756
Anais da Academia Brasileira de Ciências | *Annals of the Brazilian Academy of Sciences*
Printed ISSN 0001-3765 I Online ISSN 1678-2690
www.scielo.br/aabc | www.fb.com/aabcjournal

PALEONTOLOGY

Exploring the complex cranial morphology of *Tupandactylus imperator* (Pterodactyloidea, Tapejaridae) based on a new specimen

LUCAS CANEJO, JULIANA M. SAYÃO & ALEXANDER W.A. KELLNER

Abstract: *Tupandactylus imperator*, a striking tapejarid pterosaur from the Lower Cretaceous (Aptian) Crato Formation (Araripe Basin), is renowned for its extraordinary cranial crest, one of the proportionally largest among pterosaurs and, indeed, also among all living and extinct vertebrates. This species is known from six specimens, showing different degrees of completeness. Here we describe a new material (MN 7852-V) that represents the most complete skull and articulated lower jaw of *Tupandactylus imperator* to date, presenting an exceptionally well-preserved cranial crest composed of bone and extensive soft-tissue. Uniquely, the soft-tissue portion of the crest has a sinuous dorsoposterior margin, contrasting with previously reconstructions that suggested a convex or concave profile. The new specimen also shows several new anatomical features such as a free descending process of the nasal and several unfused elements of the lower jaw. It further displays a well-developed dentary crest and a pronounced retroarticular process, differing from previous interpretations. The specimen also displays plant material in direct contact with the mandible, which may be taphonomic or could tentatively be seen as an indication of a herbivorous feeding habit for this species.

Key words: Crato Formation, Cretaceous, Pterosauria, Tapejaridae, *Tupandactylus*.

INTRODUCTION

The richness of the pterosaur fauna in the Araripe Basin has been known for some time now, and several taxa have been described (see Pinheiro et al. 2025, for a review). Among those, the Tapejaridae, a group of toothless pterosaurs have been well represented in the Araripe Basin (Kellner 1989, Campos & Kellner 1997, Frey et al. 2003a) and the Paraná Basin (e.g., Manzig et al. 2014). Members of this clade have also been recorded in China (Wang & Zhou 2002, Zhang et al. 2019, 2023), Europe (Vullo et al. 2012) and Africa (Wellnhofer & Buffetaut 1999). Among the most interesting tapejarid features is the striking variability in the shape and size of their sagittal cranial crests (e.g., Campos & Kellner 1997, Wang & Zhou 2002, Canejo et al. 2022, Zhang et al. 2023).

Perhaps one of the most extraordinary tapejarids is *Tupandactylus imperator* (Campos & Kellner 1997) from the Lower Cretaceous (Aptian) Crato Formation (Araripe Basin). This species is known for possessing one of the largest cranial crests among flying reptiles (Campos & Kellner 1997, Pinheiro et al. 2011), and, in fact, also among all living and extinct vertebrates. When first described, the species, based on a skull lacking the lower jaw (MCT 1622-R), was initially referred to *Tapejara* (Campos & Kellner 1997) but later, reassigned to a new genus, *Tupandactylus* (Kellner & Campos 2007). Another species, originally described as *Tapejara navigans* (Frey

et al. 2003a), was also reassigned to this genus (Kellner & Campos 2007), which was followed by several subsequent studies (e.g., Pinheiro et al. 2011, Holgado et al. 2019, Beccari et al. 2021, Cerqueira et al. 2021, Pêgas et al. 2023).

All known specimens attributed to *Tupandactylus imperator* were discovered during the extraction of laminated limestone from the Crato Formation, a material widely used in the construction industry (e.g., Martill & Bechly 2007), which has been subject to several discussions (e.g., Andrade 2007, Kellner 2023, Kuhn et al. 2022). As a result of the mining activity, most of these fossils are found damaged (e.g., Pinheiro et al. 2011), lack precise geological context, and sometimes exhibit signs of artificial alteration (Martill 1994, Selden et al. 2019). To date, *Tupandactylus imperator* is represented by at least six specimens: (i) MCT 1622-R, the holotype, consisting of a complete skull lacking the lower jaw (Campos & Kellner 1997); (ii) SMNK PAL 2839, consisting of an incomplete skull (Frey et al. 2003b); (iii) an undescribed specimen that nearly preserves the entire skull, originally figured by Unwin & Martill (2007) from an private collection, and more recently donated to the Museu Nacional/UFRJ (MN 7880-V); (iv) CPCA 3590, a partially preserved skull with the first known mandible (Pinheiro et al. 2011); (v) MCT.R.1884, comprising the posterior portion of the skull (Cincotta et al. 2022); and (vi) MZSP-PV 1249, a specimen described in a doctoral thesis including an articulated skull, mandible, and partial skeleton (Piazentin, unpublished data). We tried to have access to the latter but were not successful. It should be noted that in the original figure of MN 7880-V, Unwin & Martill (2007) have wrongly labeled the scale, and that this specimen is half the size that they indicated. Another specimen, MN 6588-V, composed of postcranial elements lacking a skull, was initially identified as a possible tapejarid (Sayão & Kellner 2006) and later referred to *Tupandactylus* sp. (Beccari et al. 2021). Additionally, Pinheiro et al. (2011) briefly mention yet another material in a private collection, comprising a skull and mandible, not studied or figured so far.

Here we describe a new specimen of *Tupandactylus imperator* (MN 7852-V), to our knowledge representing the best-preserved skull and lower jaw of this species that provides new insights into the cranial anatomy, including the crest of this pterosaur.

MATERIALS AND METHODS

The specimen MN 7852-V is housed at the Museu Nacional/UFRJ (Rio de Janeiro, Brazil). It has been donated by a private collector together with other 1.103 fossils from the Araripe Basin (Kellner 2024), with the purpose of contributing to the restoration of the museum´s collection, lost in the 2018 fire (Zamudio et al. 2018, Kellner 2019). The anatomical nomenclature follows Kellner & Tomida (2000). ImageJ 1.54 (Schneider et al. 2012) software was used for large values that could not be measured with the pycnometer. Additionally, we conducted an examination under ultraviolet (UV) light at a wavelength of 365 nm, a method proven to reveal anatomical details in other vertebrate specimens with preserved soft tissue (e.g., Tischlinger & Frey 2002, Kellner et al. 2010, Lindgren et al. 2010, Hone et al. 2010, Simões et al. 2014).

Institutional abbreviations:

CPCA, Centro de Pesquisas Paleontológicas da Chapada do Araripe; MCT, Museu de Ciência da Terra; MN, Museu Nacional; MZSP, Museu de Zoologia da USP; SMNK, Staatliches Museum für Naturkunde; UFRJ, Universidade Federal do Rio de Janeiro.

SYSTEMATIC PALEONTOLOGY

PTEROSAURIA Kaup, 1834
PTERODACTYLOIDEA Plieninger, 1901
TAPEJARIDAE Kellner, 1989
Tupandactylus Kellner & Campos 2007

Emended diagnosis. Tapejarid pterosaur with the following characters: prominent, dorsally oriented supra-premaxillary process that projects anteriorly to the premaxilla and supports a soft-tissue crest; large soft-tissue sagittal crest, divided into a ventrally displaced fibrous portion with parallel fibers, and a broad area of smooth soft tissue; nasoantorbital fenestra extending approximately or exceeding 50% of the premaxilla to squamosal cranial length; and deep and rounded dentary crest.

Tupandactylus imperator (Campos & Kellner 1997)

Emended diagnosis: Tapejarid pterosaur with the following features: triangular plate formed by the premaxilla above the anterior portion of the nasoantorbital fenestra in lateral view; and an irregular height arrangement of the fibrous crest above the anterior portion of the premaxilla.

Tupandactylus imperator can be further distinguished from *Tupandactylus navigans* by having the sinuous posterior margin of the smooth soft-tissue crest, as opposed to the vertical trailing edge noted by Frey et al. (2003a) and Beccari et al. (2021). It further shows an extremely long parietal process, approximately equal in length to the premaxilla–squamosal distance, differing from the short and round condition observed in *Tupandactylus navigans* (Beccari et al. 2021). The dentary crest in lateral view of *Tupandactylus imperator* is more symmetrical, differing from the vertical posterior margin described by Beccari et al. (2021). Lastly, the ventral margin of the posterior end of the lower jaw, including the retroarticular process, is straight in *Tupandactylus imperator*, differing from the curved morphology present in *Tupandactylus navigans*.

Horizon and Locality: Crato Formation, Lower Cretaceous (Aptian), Santana Group, Araripe Basin, northeastern Brazil (see Kellner et al. 2013 for nomenclatural issues of the Santana Group). As for all specimens referred to this taxon, the exact locality where MN 7852-V was collected is unknown.

DESCRIPTION AND COMPARISON

Generalities

The specimen (MN 7852-V) is preserved on a slab that has been reassembled with adhesive (see Table I for measurements). It is composed of a skull and lower jaw exposed in right lateral view that are compressed and preserved essentially in two dimensions, contrasting with the pterosaur material preserved in the nodules of the Romualdo Formation (e.g., Kellner & Saraiva 2019). The bone surface is fragmented, showing cracks across the entire surface, a common feature in fossil tetrapods from this stratigraphic unit (Figs. 1, 2, 3). Just posterior to the orbit, the supraoccipital and part of the frontoparietal appear to be artificially painted, likely a mixture of glue and sediment, mimicking the natural coloration of the fossil that has been detected under UV light (Fig. 2).

The skull of *Tupandactylus imperator* was already described based on other specimens (Campos & Kellner 1997, Unwin & Martill 2007, Pinheiro et al. 2011, Cincotta et al. 2022, Piazentin, unpublished data). In the following description we will mainly focus on the new information that MN 7852-V provides and, where required, make the appropriate comparisons.

Table I. Measurements of the specimen MN 7852-V of *Tupandactylus imperator*.

Element	Extent	Value
Rostrum	Heights from the quadrate to the highest point of the sagittal crest.	88.63 cm
Rostrum	Rostrum height to the anterior most point of nasoantorbital fenestra.	3.32 cm
Rostrum	Rostrum height anterior to nasoantorbital fenestra.	22.83 cm
Rostrum	Inclination.	~16°
Cranium	Length from tip of premaxilla to anterior most point of nasoantorbital fenestra.	9.26 cm
Cranium	Length from tip of premaxilla to quadrate.	34.45 cm
Cranium	Length from tip of premaxilla to squamosal.	41.67 cm
Cranium	Length from tip of premaxilla to occipital crest.	70.81 cm
Cranium	Anterior process of the jugal and the lacrimal process of the jugal.	108.03°
Cranium	Anterior process of the jugal and the postorbital process of jugal.	148.88°
Cranium	Slope of the rostrum downward curvature.	157.94°
Cranium	Ventral deflection angle relative to ventral margin of the skull.	166.97°
Cranium	Ratio of the skull height / skull length.	1.25
Cranium	RV ratio *sensu* Kellner 2010; 2017.	2.79
Cranium	RI ratio *sensu* Martill & Naish, 2006.	0.41
Orbit	Height.	8 cm
Orbit	Length.	4.3 cm
Orbit	Angulation between the lacrimal process of the jugal and the postorbital process of the jugal.	41.02°
Nasoantorbital fenestra	Length.	24.35 cm
Nasoantorbital fenestra	Height.	9.57 cm
Nasoantorbital fenestra	Ratio of nasoantorbital fenestra length / height.	2.54
Lower jaw	Length from tip of dentary to retroarticular process.	35.85 cm
Lower jaw	Height of the mandibular ramus.	2.24 cm
Lower jaw	Height of the dentary crest.	10.7 cm
Lower jaw	Length of the dentary crest.	15.88 cm
Lower jaw	Ventral deflection angle relative to dorsal margin of the mandible.	107.35°
Lower jaw	Length of retroarticular process.	2.54 cm
Lower jaw	Ratio of the dentary crest height / mandibular ramus height *sensu* Vullo et al. 2012.	4.77
Lower jaw	Ratio of the dentary crest height / dentary crest length.	0.49

Skull

As usual in most pterodactyloids, the largest opening of the skull is the nasoantorbital fenestra, that in MN 7852-V is elliptical, longer than in *Tupandactylus navigans* (see Frey et al. 2003a) and comprises 34.38% of the total length of the skull (measured from the tip of the premaxilla to the posterior end of the parietal crest) and 58.4% of the premaxilla to squamosal length, a proportion comparable to

Figure 1. Photograph of the new specimen of *Tupandactylus imperator* (MN 7852-V) showing details of the fibers in the fibrous crest. Scale bar = 10 cm; detailed figures scales = 5 mm.

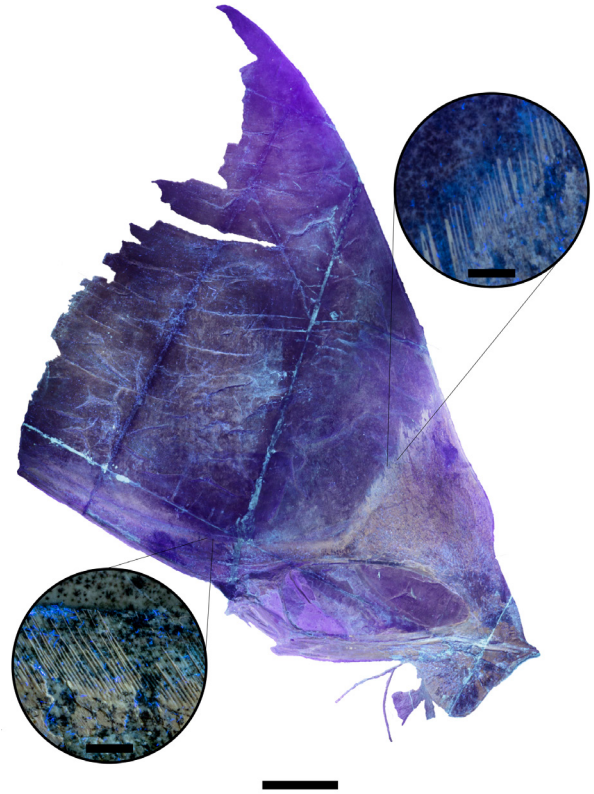

Figure 2. Photograph of the new specimen of *Tupandactylus imperator* (MN 7852-V) under ultraviolet light with a wavelength of 365 nm showing details of the fibers in the fibrous crest. Scale bar = 10 cm; detailed figures scales = 5 mm.

those observed in other specimens, such as 59% in MCT 1622-R (holotype) (Campos & Kellner 1997) and ~60% in MN 7880. In contrast, these values are slightly higher than those recorded for *Tupandactylus navigans*, which are ~50% in SMNK 2344 PAL, ~49% in SMNK 2343, and 45% in GP/2E 9266 (Beccari et al. 2021). *Tapejara wellnhoferi* and *Sinopterus dongi* show even lower proportions, of ~43 and 41.7% respectively (Wellnhofer & Kellner 1991, Wang & Zhou 2002).

The orbit is piriform and has a small bone interpreted as part of the sclerotic ring. The lower temporal fenestra is reduced, slit-like, as in all known *Tupandactylus* skulls where the posterior portion is preserved.

The maxilla and premaxilla are completely fused. In lateral view, the ventral margin formed by the maxilla and jugal under the nasoantorbital fenestra is slightly concave somewhat following the dorsal margin of the dentary. Starting close to the anterior margin of the nasoantorbital fenestra, the ventral margin of the skull formed by the maxilla-premaxilla is inclined, with the ventral portion of the rostral end forming an angle of ~16° relative the horizontal margin. Based on the known specimens of *Tupandactylus imperator*, this inclination varies from ~12° of MCT 1622-R (holotype), ~15 of CPCA 3590 (Pinheiro et al. 2011), and ~20° of the MN 7880-V. Comparable values are observed in *Tupandactylus navigans*, ranging from ~16° in SMNK 2343, ~22° in SMNK 2344 PAL (holotype), and ~21° in GP/2E 9266.

Anteriorly, the premaxilla tapers into a pointed tip. In lateral view, the ventral margin

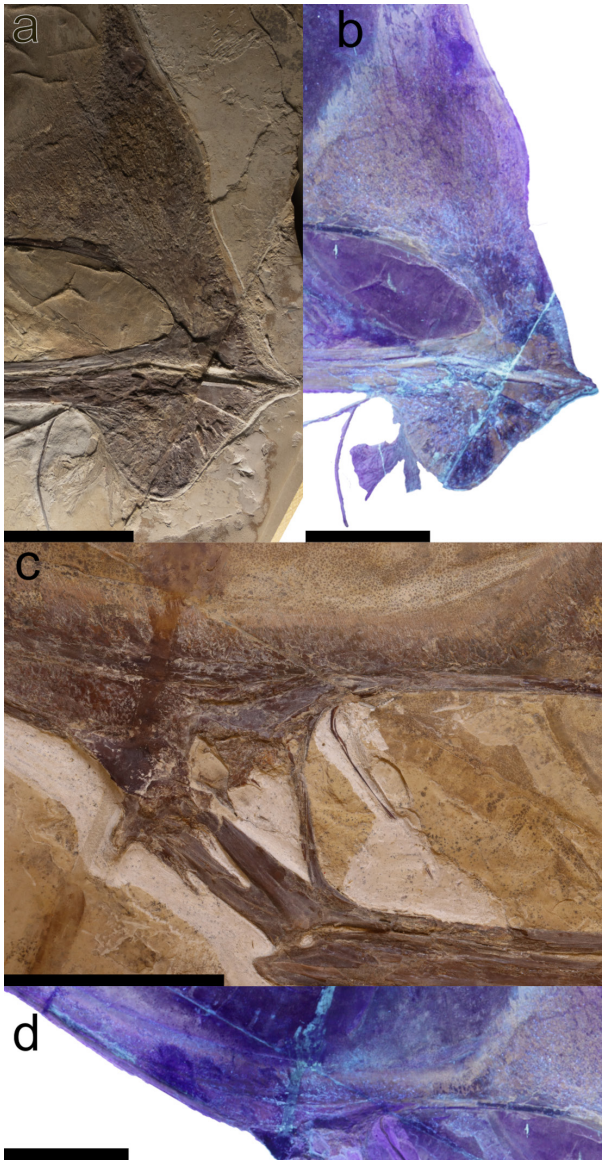

Figure 3. ***Tupandactylus imperator*** **(MN 7852-V). (a, b) Photographs of the anterior portion of the skull, including the premaxilla and lower jaw, under visible light and ultraviolet light (365 nm), respectively; (c) photograph of the posterior region of the skull in right lateral view; (d) photograph of the posterior portion of the skull under ultraviolet light (365 nm), including the frontal, part of the parietal crest, and the supraoccipital crest. Note the brighter regions under ultraviolet light, revealing a mixture of glue and sediment used to mimic the original fossil coloration. Scale bar = 10 cm.**

of the rostrum is sightly curved, indicating the presence of a small gap between both jaws, this is found in other tapejarid pterosaurs, where it is more developed (e.g., Wellnhofer & Kellner 1991). The palatal region is not visible due to both the lateral compression of the specimen and the proximity of the lower jaw, which is articulated with the skull. At the anterior portion there are some bone fragments that most likely are part of the palatal region but are too incomplete to provide any particular anatomical feature.

There is a lighter colored portion anterior to the bony part of the premaxillary crest that is here interpreted as the remains of a rhamphotheca. This structure, probably formed by keratinized epidermis, stops at the anterior protuberance of the premaxillary crest. It is also present in the lower jaw, where it forms the anterior margin of the dentary crest. The rhamphotheca of MN 7852-V seems to correspond to the "rostral crest" of *Tupandactylus navigans* SMNK PAL 2344 (Frey et al. 2003a) and differs by being comparatively reduced in this specimen of *Tupandactylus imperator*. In GP/2E 9266 of *Tupandactylus navigans*, the rhamphotheca is also more developed than in MN 7852-V (Beccari et al. 2021), which may represent a potential phylogenetic signal or alternatively could be taphonomic.

Laterally, the anterior margin of the premaxillary crest is irregular, starting slightly concave until changing to slightly convex, forming an anterior bump. Towards the posterior region, the premaxillary expands into a triangular bony plate extending approximately halfway along the length of the nasoantorbital fenestra, a condition observed in all specimens attributed to this species where this region is preserved (MCT 1622-R, CPCA 3590, and MN 7880-V). In both specimens of *Tupandactylus navigans* (SMNK 2344 PAL and GP/2E 9266), although there is also an anterior bony expansion of the crest, it does not expand posteriorly (Frey et al. 2003a, Beccari et al. 2021).

The posterior process of the premaxilla extends the full length of the parietal crest, maintaining continuous contact with the frontoparietal but does not fuse with it, with a gap perceptible at the most posterior portion. This has also been observed in closely related pterosaurs (e.g., *Tapejara wellnhoferi*, *Sinopterus dongi*, *Caiuajara dobruskii*, *Meilifeilong sanyainus*, and *Meilifeilong youhao*), where, however, the separation between these bones is larger (Wellnhofer & Kellner 1991, Wang & Zhou 2002, Canejo et al. 2022, Ji et al. 2023, Wang et al. 2023). The supra-premaxillary process marks the anterior edge of the sagittal crest, with a slightly posterior inclination, differing from the more verticalized condition observed in *Tupandactylus navigans* (Frey et al. 2003a). In GP/2E 9266 this process is even oriented anteriorly (Beccari et al. 2021) what could be taphonomic.

The nasal is a triangular triradiate structure presenting an elongated thin free nasal process. In lateral view, its dorsal margin displays a convex curvature and occupies the posterodorsal margin of the nasoantorbital fenestra (Figs. 3c, 4). A sharply projecting anterior process mirrors the morphology observed in specimen CPCA 3590 (Pinheiro et al. 2011). From the posterior half of the nasal originates a slender descending process that initially curves anteriorly before straightening and extending 8.2 cm inside the nasoantorbital fenestra. Both right and left descending process exhibit posterior inclination, though dorsal fracturing has accentuated this angulation. This configuration closely resembles the holotype (SMNK 2344 PAL) of *Tupandactylus navigans* (Frey et al. 2003a), but in the new *Tupandactylus imperator* specimen (MN 7852-V) is longer and more inclined anteriorly, likely differences that might be attributed to preservation. Perhaps the configuration of the nasal process, which differs from all other pterosaurs but shows some similarities with the chaoyangopterid *Meilifeilong youhao* (see Wang et al. 2023), represents a potential phylogenetical signal.

The posterior process of the nasal contacts the dorsal margin of the orbit, while its concave ventral margin contacts the dorsal and anterior margin of the lacrimal - a condition also observed in *Tapejara wellnhoferi* (Wellnhofer & Kellner 1991).

The frontal exhibits several distinct fissures, with adhesive visible where fragments were reassembled (Figs. 1, 2, 3d). This element shows moderate distortion, revealing portions of the internal surface of the orbit. No discernible sutures separate the frontal from the parietal. The frontal forms most of the orbit dorsal margin and extends anteriorly to broadly overlap the nasal, creating an elongated anterior process (Fig. 4). This morphology parallels that observed in other tapejarids, including *Eopteranodon yixianensis*, *Tapejara wellnhoferi*, and *Sinopterus dongi* (Wellnhofer & Kellner 1991, Wang & Zhou 2002, Zhang et al. 2023). In lateral view, the process displays a convex dorsal margin.

The frontoparietal constitutes the primary structural component of the internal surface of the upper temporal fenestra. Posterior to the fenestra, the parietal articulates with the supraoccipital in the occipital region. The parietal crest shows remarkable posterior elongation, accounting for approximately half of the total skull length – a feature also observed in other specimens (e.g., Campos & Kellner 1997, Pinheiro et al. 2011). It shows a thicker, rod-like ventral portion that articulates with the supraoccipital, extending the length of the crest with a constant height of 8.5 mm along the anteroposterior axis. Dorsally, the crest is considerably more fragile, narrowing posteriorly. This region extends parallel to the premaxillary process.

The lacrimal exhibits extensive fenestration, a feature shared with other

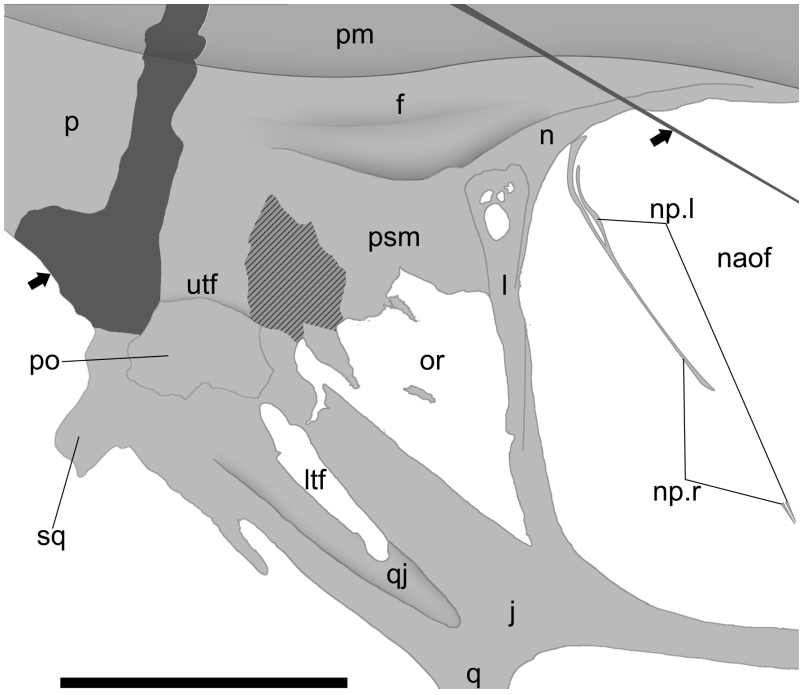

Figure 4. ***Tupandactylus imperator*** **(MN 7852-V), schematic drawing of the bones that make up the posterior region of the skull, in right lateral view. Abbreviations: f, frontal; j, jugal; l, lacrimal; ltf, lower temporal fenestra; n, nasal; naof, nasoantorbital fenestra; np, free nasal processes from both sides; or, orbit; p, parietal; pm, premaxilla; po, postorbital; psm, pseudomesethmoid; qj, quadratojugal; sq, squamosal; utf, upper temporal fenestra. Bold arrows indicate broken areas filled with glue and limestone, and hatched areas indicates regions where the external bone surface was lost. Scale bar = 5 cm.**

tapejarids (e.g., Wellnhofer & Kellner 1991, Wang & Zhou 2002, Canejo et al. 2022, Zhang et al. 2023). This triangular element displays marked dorsoventrally elongation, measuring approximately 49 mm in height and 12 mm in anteroposterior length. It constitutes the primary component of the anterior margin of the orbit. Although the ventral limit of this bone is poorly preserved, the lacrimal extends parallel to the dorsal process of the jugal, ending about 15 mm above the ventral margin of the orbit. This morphology contrasts with the dorsally expanded condition observed in *Tapejara wellnhoferi*, *Sinopterus dongi*, and *Caiuajara dobruskii* (Wellnhofer & Kellner 1991, Wang & Zhou 2002, Canejo et al. 2022) but closely resembles that of *Tupandactylus navigans* (Beccari et al. 2021).

The postorbital presents a triangular morphology and articulates posteriorly with the frontoparietal, anteriorly with the jugal, and ventrally with the squamosal, similar to other pterodactyloid taxa (e.g., Wellnhofer & Kellner 1991, Bennett 2001, Wang & Zhou 2002, Wang et al. 2023). The frontal process is fractured, revealing the internal surface of the upper temporal fenestra. Additionally, the postorbital contributes to the posterior margin of the lower temporal fenestra, which shows moderate distortion along its dorsal edge where it contacts the postorbital process from the jugal.

The jugal is a triradiate element showing the same morphological traits that are consistent with other tapejarids (e.g., Beccari et al. 2021, Canejo et al. 2022). Its anterior process, extending approximately 170 mm into the ventral margin of the nasoantorbital fenestra, exhibits a medial fracture with substantial loss of the external surface of the bone. The dorsal process maintains a subvertical orientation at ~108° relative to the anterior process, similar to the typical tapejarid condition (e.g., Kellner 1989, 2013, Wang & Zhou 2002).

The right quadrate is visible only in lateral view, where it articulates with the lower jaw and extends 65 mm posteriorly, contacting with the squamosal and dorsally the quadratojugal. It forms an angle of 141° relative to the maxilla,

which is comparable to the approximately 150° observed in the holotype of *Tupandactylus imperator* and the 148° reported for specimen GP/2E 9266 of *Tupandactylus navigans* (Beccari et al. 2021). The quadratojugal extends 59 mm posteriorly, articulating dorsally with the jugal and ventrally with the quadrate. It contributes to forming the anterior and ventral margins of the lower temporal fenestra. The squamosal is an elongated element measuring approximately 49 mm in length, it has little contribution to the posterior margin of the lower temporal fenestra (Fig. 4). It possesses an anteroventraly oriented otic process that forms a narrow notch with smooth, rounded interior surface. This morphology shows subtle differences from the tapejarine *Tapejara* (Wellnhofer & Kellner 1991), while resembling the pteranodontoid *Pteranodon* (Bennett 2001). Notably, it contrasts with the short and broad condition observed in the chaoyangopterid *Meilifeilong youhao* (Wang et al. 2023). Posteriorly, the squamosal extends ventrally into a developed tuberosity. According to Bennett (2001), these structures would support the tympanic region of the ear and serve as an attachment site for the *M. depressor mandibulae* and/or axial muscles, respectively. This configuration results in an "L"-shaped squamosal. The postorbital overlaps the squamosal dorsally. Posteriorly, the squamosal contacts the frontoparietal with no clear suture, while anteriorly it overlaps the posteroventral surface of the quadrate. The occipital region is covered by the matrix.

Mandible

The lower jaw is preserved articulated with the skull. The mandibular ramus displays a longitudinal fissure along its long axis, with partially discernible element boundaries posteriorly. The bone surface at the anterior margin of the dentary crest is brighter than the rest of the crest and most likely was covered by keratinous soft-tissue structure, forming a rhamphotheca (Figs. 1, 2). Posteroventral of the dentary crest there are some filamentous structures that are regarded as plant remains. As in all members of the Tapejaridae, jaws are toothless.

As characteristic in pterosaurs, for all in the Pterodactyloidea, the dentary is the main bone of the mandible, extending posteriorly until the retroarticular process, overlapping the angular (Figs. 5a, b). On the ventral portion of the anterior end, there is a well-developed and deep dentary sagittal crest, with the ratio of the crest height (dc-h) relative to the height of the mandibular ramus (mr-h) (*sensu* Vullo et al. 2012) of 4.77 (dc-h/mr-h) (Fig. 6a). This value exceeds those of *Tupandactylus imperator* CPCA 3590 (dc-h/mr-h ~3) (Fig. 6b), *Europejara olcadesorum* (dc-h/mr-h ~4) (Vullo et al. 2012), *Tapejara wellnhoferi* (dc-h/mr-h ~2.5), *Sinopterus dongi* (dc-h/mr-h ~2.2), and *Caiuajara dobruskii* (dc-h/mr-h 1.6-1.8) (Canejo et al. 2022), but is lower than in *Tupandactylus navigans* (dc-h/mr-h 5.3) (Beccari et al. 2021) (Fig. 6c). The maximum length of the dentary crest comprises 44% of the total length of the lower jaw compared to 51% of CPCA 3590 (Pinheiro et al. 2011). This proportion is similar to that observed in *Tupandactylus navigans*, which shows ~45% in GP/2E 9266 (Beccari et al. 2021).

Due to preservation, the length of the symphysis cannot be precisely determined. The anterior region of the symphysis is downturned, and the dorsal margin is slightly concave, suggesting the presence of a gap between the jaws, as already observed in the upper jaw. In the specimen CPCA 3590 (Pinheiro et al. 2011), the concavity is even more pronounced (Fig. 6b).

The specimen exhibits a well-developed retroarticular process, measuring 2.54 cm in length, corresponding to approximately 7% of the length of the mandibular ramus. This proportion

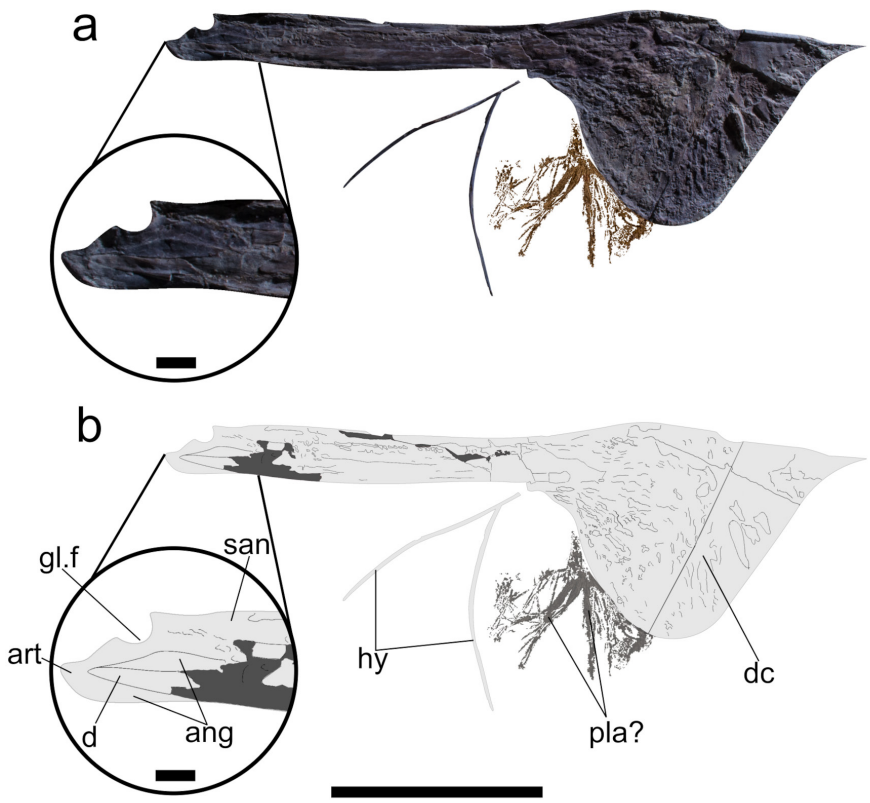

Figure 5. ***Tupandactylus imperator*** **(MN 7852-V), lower jaw in right view. (a) edited photo with matrix removed for clarity with details of the posterior end of the mandibular ramus; (b) schematic drawing, with details of the posterior end of the mandibular ramus. Note the probable plant material positioned ventroposteriorly to the dentary crest. Abbreviations: ang, angular; art, articular; d, dentary; dc, dentary crest; gl.f, glenoid fossa; hy, hyoid bones; pla?, possible plant material; san, surangular. Scale bar = 10 cm; detailed figure scale = 1cm.**

matches that observed in *Aymberedactylus cearensis* and *Tupandactylus navigans* (Pêgas et al. 2016, Pinheiro et al. 2011, Beccari et al. 2021) but contrasts with previous interpretation of sole other lower jaw from *Tupandactylus imperator* (CPCA 3590).

The surangular is an elongated rectangular element forming the dorsal margin of the posterior end of the mandibular ramus. Although the anterior limits with the dentary are not clear due to the broken condition of the external bone surface, this bone is clearly surrounded anteriorly and ventrally by the dentary and posteriorly overlaps the angular. Posteriorly, it participates in the glenoid fossa.

The angular is an elongated bone that constitutes the ventral margin of the posterior end of the mandibular ramus. Dorsally, it is overlapped by the posterior end of the dentary and contacts the surangular. Its posterior contact with the articular lacks a visible suture. The angular likely contributes to the lateral surface of the retroarticular process.

The articular is a small bone apparently fused with the surrounding elements. In lateral view, it participates in the glenoid fossa and forms the majority of the retroarticular process (Fig. 5).

Hyoid bone

Two thin and elongated elements that are fused anteriorly can be observed ventral to the mandible (Fig. 5). They are interpreted and being both ceratobranchials. Despite the evident deformation, their shape resembles the condition observed in other pterosaurs, without any special anatomical features, similar to *Tapejara wellnhoferi* and *Ludodactylus sibbicki* (Wellnhofer & Kellner 1991, Frey et al. 2003c).

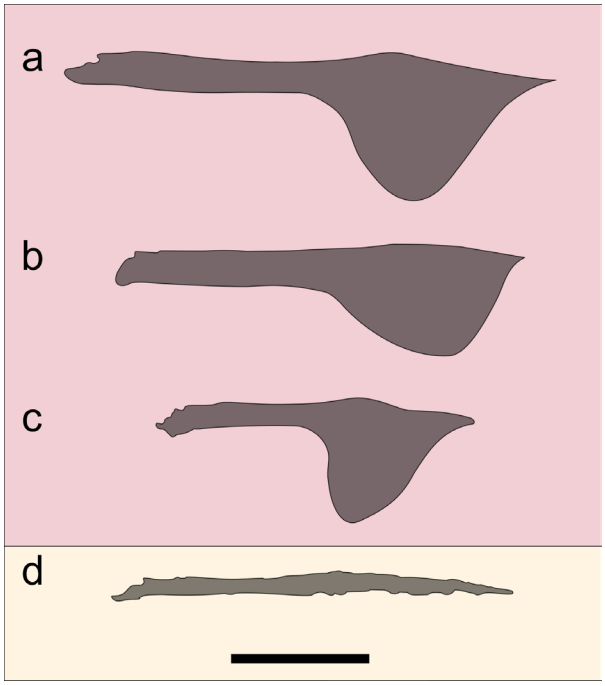

Figure 6. Silhouette of the lower jaws of known specimens of *Tupandactylus* (a - c) and *Aymberedactylus* (d). (a) MN 7852-V, *T. imperator*; (b) CPCA 3590 (inverted), *T. imperator* (based on Pinheiro et al. 2011); (c) GP/2E 9266 (inverted), *T. navigans* (based on Beccari et al. 2021); (d) MN 7596-V, *Aymberedactylus cearensis* (based on Pêgas et al. 2016). Scale bar = 10 cm.

However, available data on the hyoid apparatus in pterosaurs, remains limited (Jiang et al. 2020).

Soft tissue crest

The soft tissue sagittal crest of *Tupandactylus* comprises two distinct regions: a ventrally displaced fibrous crest and a smooth, broad dorsal region (Beccari et al. 2021), hereafter termed the 'smooth crest'. Although the posterodorsal portion of the smooth crest lacks a defined dorsal margin, its overall morphology remains discernible. In specimen MN 7852-V, the fibrous crest exhibits subtle fluorescence differences when compared to both the bony crest and the smooth crest (Fig. 2). Anteriorly, the fibrous crest originates at the bony premaxillary crest and extends posteriorly, closely following the dorsal skull in lateral view. This condition is also observed in other specimens of *Tupandactylus imperator* and *Tupandactylus navigans*. The fibers are anchored along the premaxilla's long axis (Figs. 1, 2), gradually thinning as they extend dorsally to connect with the soft crest. Ventrally, these fibers measure approximately 0.33 mm in length. Along their anteroposterior distribution, the fibers range in height from 0.5 cm to 1.3 cm (mean ~0.9 cm), with the anterior fibers being slightly longer on average (~1.3 cm to 0.6 cm) and becoming slightly shorter posteriorly, toward the triangular plate (0.5 cm to 0.9 cm) (Fig. 1). The fibers exhibit an average density of 26 fibers per centimeter along the entire anteroposterior extension of the premaxilla. Anteriorly, their arrangement is irregular, forming an uneven fibrous crest dorsal to the triangular plate of the premaxilla - a pattern contrasting with the apparently more organized dorsoventral arrangement observed in *Tupandactylus navigans* (Frey et al. 2003a). Posteriorly, the fibers become progressively more regular, tapering along the premaxillary process. Near the distal end of the premaxillary process, the fibers adopt a more inclined orientation, aligning almost horizontally relative to the parietal process, with the longest fibers occurring in this region.

The sagittal crest extends predominantly dorsally rather than posteriorly, differing from earlier interpretations based on initial specimens (Campos & Kellner 1997, Pinheiro et al. 2011). The posterior margin of the smooth soft tissue crest retains a sinuous appearance, with a convex lower half and a concave upper half, forming an inverted S-shape. A comparable morphology is observed in specimen MCT.R.1884 (Cincotta et al. 2022).

Plant material

Posteroventral to the dentary crest, several filamentous structures can be identified (Fig. 5).

There clearly are not bone structures neither part of soft tissue of this pterosaur. They are also not gastric pellets or coprolites, that have occasionally been recorded with pterosaur remains (see Jiang et al. 2022). These fibers are wider and more compact in the region closest to the mandible and become narrow and frayed further from the dentary crest. There is no other evidence of this type of structure in other parts of this specimen, neither in the cranial part nor in other parts of the calcareous plate. They are here interpreted as partially decomposed plant remains.

DISCUSSION

Campos & Kellner (1997) were the first to describe the sagittal crest of *Tupandactylus imperator*, distinguishing it into two components: a bony crest, primarily formed by the premaxilla, and a soft tissue crest. According to Beccari et al. (2021), the soft tissue crest of *Tupandactylus* is divided into two main regions: the ventrally displaced fibrous crest and a wider, smooth dorsal portion. In both *Tupandactylus imperator* and *Tupandactylus navigans*, the fibrous crest originates in the anterior bony premaxillary crest, extending posteriorly along the dorsal margin of the skull. Due to morphological differences in both the premaxilla and skull dorsal margin, the fibrous crest exhibits two distinct morphologies in lateral view. In *Tupandactylus navigans*, the bony premaxillary crest and the supra-premaxillary process form an almost perpendicular angle to the ventral margin of the skull, as observed in specimen GP/2E 9266 (Beccari et al. 2021). This morphology is associated with two distinctive features: a short parietal crest that creates an L-shaped fibrous crest (Frey et al. 2003a, Beccari et al. 2021), and a regular dorsoventral arrangement that tapers posteriorly with a vertical and sub-parallel displacement of the fibers (Beccari et al. 2021). This morphology differs from that observed in *Tupandactylus imperator* (MN 7852-V), particular regarding its posterior extension. The differences are primarily related to the development of the bony premaxillary crest and the presence of a well-developed parietal crest. Pinheiro et al. (2011) argue that the fibers observed in *Tupandactylus imperator* underwent mineralization along the dorsal margin of the premaxilla, penetrating the bone, which is also observed for *Tupandactylus navigans*, and *Tupandactylus imperator* (MN 7852-V). The dorsoposterior limit of the soft tissue crest in *Tupandactylus imperator* has been a subject of continuous debate over the years (e.g., Campos & Kellner 1997, Pinheiro et al. 2011, Cincotta et al. 2022). The initial interpretation proposed a sail-like crest with a concave posterior margin (Campos & Kellner 1997). Pinheiro et al. (2011), based on a more complete specimen illustrated by Unwin & Martill (2007) and CPCA 3590 - considered the best-preserved individual for the species at the time –, argued that the shape was rounded with a convex posterior margin. The sinuous morphology of the posterior limit of the soft tissue crest observed in specimen MN 7852-V, as described here, is also present in MCT.R.1884, an exquisite individual that preserves the posterior portion of the skull, including the dorsoposterior limit of the soft crest. Such a specimen was used to document the presence of melanosomes in this pterosaur (Cincotta et al. 2022). And although only minimal description of the posterior limit of the soft tissue crest was provided, it is evident that the structure was neither completely concave or convex, contrary to the interpretations of previous authors (Campos & Kellner 1997, Pinheiro et al. 2011) (Fig. 7). Instead, it displays a ventrally convex region and a dorsally concave area. Despite considerable distortion, primarily due to the dorsal curvature of the parietal crest and the posterior curvature of the premaxillary dorsal process - which exaggerate the sinuosity

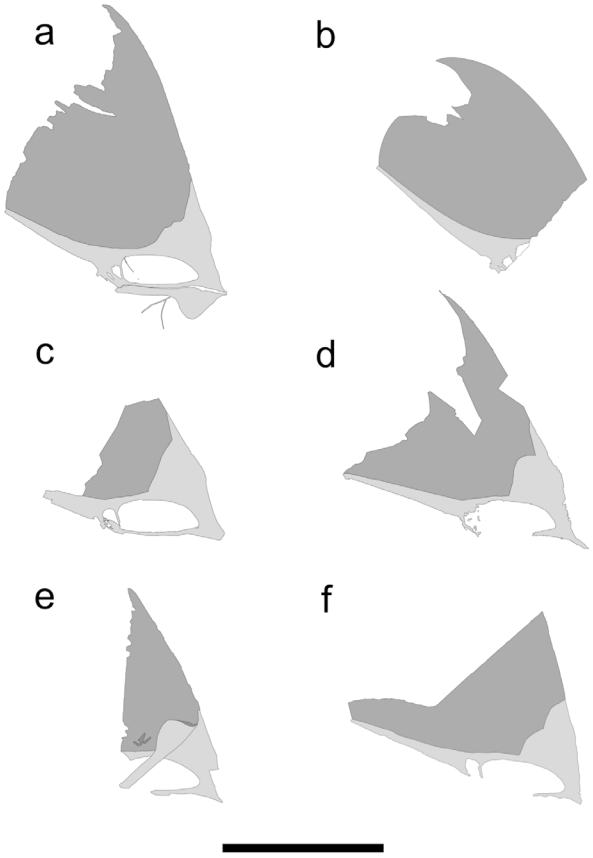

Figure 7. Schematic drawings showing the outline of different specimens referred to *Tupandactylus imperator*, all preserving at least part of the soft tissue portion of the cranial crest. (a) MN 7852-V; (b) MCT.R.1884 (inverted, based on Cincotta et al. 2022); (c) MCT 1622-R (holotype), left slab; (d) MCT 1622-R (holotype), right slab (inverted) (based on Campos & Kellner 1997); (e) CPCA 3590 (based on Pinheiro et al. 2011); (f) MN 7880-V (based on Unwin & Martill 2007 with corrected scale bar proportions). Scale bar = 50 cm.

-, this interpretation remains valid. Furthermore, the soft crest of specimen MN 7852-V, as described here, is more developed dorsally than posteriorly due to the greater dorsal extension of the supra-premaxillary process compared to the posterior extension of the parietal crest. This morphology probably caused the soft crest to be slightly stretched in life, resulting in a subtle sinuosity.

Regarding the lower jaw, the sole described one attributed to *Tupandactylus imperator* (CPCA 3590) is rather incomplete, for all the posterior region (Pinheiro et al. 2011). The new specimen (MN 7852-V) shows that the dentary crest is more symmetric in lateral view than previously observed in CPCA 3590 (Figs. 6a, b). This condition differs from GP/2E 9266 attributed to *Tupandactylus navigans* (Beccari et al. 2021), which exhibits an almost vertical posterior margin (Fig. 6c). Additionally, *Tupandactylus navigans* shows the posterior end of the lower jaw curved downward, similar to the condition observed in *Aymberedactylus cearensis*.

The new specimen provides more information regarding the posterior portion of the mandible (Figs. 5a, b). In MN 7852-V the retroarticular process is well developed, similar to *Tupandactylus navigans* and *Aymberedactylus cearensis*. While some authors proposed *Aymberedactylus* (Fig 6d) as a junior synonym of *Tupandactylus* (Martill et al. 2018), this hypothesis lacks substantial supporting evidence and has not gained acceptance over the years. Notably, *Aymberedactylus* shares the downward-curved retroarticular process morphology with *Tupandactylus navigans* (GP/2E 9266) (Figs. 6c, d). Unfortunately, the holotype of *Aymberedactylus* (MN 7596-V) suffered damage during the 2018 Museu Nacional/UFRJ fire. The material was recovered from the debris and is currently undergoing stabilization procedures.

There are few morphological differences among the *Tupandactylus imperator* specimens such as the size of the dentary crest and the extension of the premaxillary crest (Fig. 6). These features might reflect ontogenetic variation, with CPCA 3590 representing a smaller individual compared to MN 7852-V.

Lastly, there are some filamentous materials preserved ventroposteriorly to the dentary crest, that are being interpreted as possible plant remains. The association of plants and pterosaurs has not been commonly reported. In one case from the same Crato Formation, a leaf was found

within the mandibular rami of *Ludodactylus sibbicki*, that has been regarded as the *causa mortis* of this individual (Frey et al. 2003c). The leaf can be referred to welwitschia-like gymnosperm plant quite commonly found in the laminated limestone layers of the Crato Formation. Although it is not clear if this leave has anything to do with the pterosaur death, it should not have been part of the diet of *Ludodactylus*, that might have preyed on fish. However, most recently there have been phytoliths in the stomach content of a Tapejaridae pterosaur from China (Jiang et al. 2025). Although this association in MN 7852-V could be a taphonomic artifact, as seems to be case of *Ludodactylus*, it is tempting to regard *Tupandactylus imperator* as herbivorous as previouly suggested for *Tupandactylus navigans* (Beccari et al. 2021) and other tapejarids (Pêgas et al. 2021). More information, however, is necessary to confirm this hypothesis.

CONCLUSIONS

The new specimen MN 7852-V represents the most complete and best-preserved skull, including the lower jaw, of *Tupandactylus imperator* known to date, shedding new light on the cranial anatomy of this species. Unlike previous specimens, the preservation of the new material reveals a sinuous dorsoposterior margin in the soft-tissue portion of the crest, contrasting with earlier reconstructions that depicted this region as either concave (Campos & Kellner 1997) or convex (Pinheiro et al. 2011). MN 7852-V indicates that the cranial crest is higher than long and shows an irregular layer composed of fibrous structures between the bony and soft tissue portion of the cranial crest. These fibers, which are clearly discernible with ultraviolet light differ from the fibrous arrangement observed in *Tupandactylus navigans* by being shorter and subvertical (i.e., and not dorsoposteriorly inclined). The new specimen also shows the limits between the posterior bones that form the lower jaw, with a well-developed retroarticular process.

Although not conclusive, the association a plant remain with the lower jaw of this specimen can be interpreted as a taphonomic artifact, but it can also be viewed, with caution, as evidence that may indicate herbivory in *Tupandactylus* (Fig. 8).

Figure 8. Life reconstruction of *Tupandactylus imperator* based on specimen MN 7852-V, in the paleoenvironment of the Crato Formation. Artwork by Maurilio Oliveira.

Acknowledgments

The authors would like to thank Handerson da Silva and Ana Luiza Castro do Amaral (Central Laboratory of Conservation and Restoration - MN/UFRJ) for their support with photography and access to the material, as well as Helder de Paula Silva (Paleovertebrate Laboratory MN/UFRJ) for the additional preparation of the specimen. Mariana Rocha (Meteoritic Sector MN/UFRJ) is thanked for her support with the XRF analysis. LC thanks João Kaiuca (MN/UFRJ) for discussions on earlier versions of the manuscript. The authors acknowledge Burkhard Pohl and Rüdiger Pohl for donating the specimen and Frances Reynolds from the Instituto Inclusartiz for the partnership in supporting the reconstruction of the collection of the Museu Nacional/UFRJ. This study was funded by the Conselho Nacional de Desenvolvimento Científico e Tecnológico (CNPq #308707/2023-0, #406779/2021-0, INCT PALEOVERT #406902/2022-4 to AWAK, #309245/2023-0 to JMS, #141114/2023-1 to LC), the Fundação Carlos Chagas Filho de Amparo à Pesquisa do Estado do Rio de Janeiro (FAPERJ #E-26/210.066/2023 and #E-26/204.280/2024 to JMS; #E-26/201.095/2022 to AWAK).

REFERENCES

ANDRADE JAFG. 2007. Commercial exploitation of the Crato Formation. In: Martill DM, Bechly G & Loveridge RF (Eds), The Crato Fossil Beds of Brazil—Window into an Ancient World, Cambridge: Camb Univ Press, p. 63-69.

BECCARI V, PINHEIRO FL, NUNES I, ANELLI LE, MATEUS O & COSTA FR. 2021. Osteology of an exceptionally well-preserved tapejarid skeleton from Brazil: Revealing the anatomy of a curious pterodactyloid clade. PLoS ONE 16(8): e0254789.

BENNETT SC. 2001. The osteology and functional morphology of the Late Cretaceous pterosaur *Pteranodon*. Schweiz Verlagsbuchhandlung, p. 1–112.

CAMPOS D & KELLNER AWA. 1997. Short note on the first occurrence of Tapejaridae in the Crato Member (Aptian), Santana Formation, Araripe Basin, northeast Brazil. An Acad Bras Cienc 69: 83-87.

CANEJO L, HOLGADO B, WEINSCHÜTZ LC, RICETTI JH, WILNER E & KELLNER AWA. 2022. Novel information on the cranial anatomy of the tapejarine pterosaur *Caiuajara dobruskii*. PLoS ONE 17(12): e0277780.

CERQUEIRA GM, SANTOS MAC, MARKS MF, SAYÃO JM & PINHEIRO FL. 2021. A new azhdarchoid pterosaur from the Lower Cretaceous of Brazil and the paleobiogeography of the Tapejaridae. Acta Palaeontol Pol 66(3): 555-570 doi:https://doi.org/10.4202/app.00848.2020.

CINCOTTA A ET AL. 2022. Pterosaur melanosomes support signaling functions for early feathers. Nature 604: 684-688.

FREY E, MARTILL DM & BUCHY MC. 2003a. A new species of tapejarid pterosaur with soft-tissue head crest. Geol Soc Lond Spec Publ 217: 65-72.

FREY E, MARTILL DM & BUCHY MC. 2003c. A new crested ornithocheirid from the Lower Cretaceous of northeastern Brazil and the unusual death of an unusual pterosaur. Geol Soc Lond Spec Publ 217: 55-63.

FREY E, TISCHLINGER H, BUCHY MC. 2003b. New specimens of Pterosauria (Reptilia) with soft parts with implications for pterosaurian anatomy and locomotion. Geol Soc Lond Spec Publ 217: 233-266.

HOLGADO B, PÊGAS RV, CANUDO JI, FORTUNY J, RODRIGUES T, COMPANY J & KELLNER AWA. 2019. On a new crested pterodactyloid from the Early Cretaceous of the Iberian Peninsula and the radiation of the clade Anhangueria. Sci Rep 9(1): 4940.

HONE DWE, TISCHLINGER H, XU X & ZHANG F. 2010. The extent of the preserved feathers on the four-winged dinosaur *Microraptor gui* under ultraviolet light. PLoS ONE 5(2): e9223.

JI S, ZHANG L & LU F. 2023. A new species of chaoyangopterid pterosaur from the Early Cretaceous in western Liaoning, People's Republic of China. Acta Geol Sin 97: 1723-1740.

JIANG S, LI Z, CHENG X & WANG X. 2020. The first pterosaur basihyal, shedding light on the evolution and function of pterosaur hyoid apparatuses. PeerJ 8: e8292.

JIANG S, WANG X, ZHENG X, CHENG X, WANG X, WEI G & KELLNER AWA. 2022. Two emetolite-pterosaur associations from the Late Jurassic of China, showing the first evidence for antiperistalsis in pterosaurs. Phil Trans Royal Soc B 377: 20210043. https://doi.org/10.1098/rstb.2021.0043.

JIANG S, ZHANG X, WUA Y, ZHENG M, KELLNER AWA & WANG X. 2025. First occurrence of phytoliths in pterosaurs - evidences for herbivory. Science Bulletin: DOI 10.1016/j.scib.2025.06.040.

KELLNER AWA. 1989. A new edentate pterosaur of the Lower Cretaceous from the Araripe Basin, Northeast Brazil. An Acad Bras Cienc 61: 439-446.

KELLNER AWA. 2013. A new unusual tapejarid (Pterosauria, Pterodactyloidea) from the Early Cretaceous Romualdo Formation, Araripe Basin, Brazil. Earth Environ Sci Trans R Soc Edinb 103(3–4): 409-421.

KELLNER AWA. 2019. A reconstrução do Museu Nacional: bom para o Rio, bom para o Brasil. Ciênc Cult 71: 4-5.

KELLNER AWA. 2023. Fósseis, leis e bom senso. Mesa redonda: Descolonização da Paleontologia Brasileira (SBPC). Anais: da 74ª Reunião Anual da SBPC (2022), Sociedade Brasileira para o Progresso da Ciência, São Paulo. https://reunioes.sbpcnet.org.br/74RA/PDFs/arq_2559_599.pdf; p.1-5; ISSN 2176-1221.

KELLNER AWA. 2024. An exceptional donation. In: Museu Nacional - The reconstruction journey, p. 9-11. Inclusartiz.

KELLNER AWA & CAMPOS D. 2007. Short note on the ingroup relationships of the Tapejaridae (Pterosauria, Pterodactyloidea). Bol Mus Nac 75: 16.

KELLNER AWA, CAMPOS DA, SAYÃO JM, SARAIVA AAF, RODRIGUES T, OLIVEIRA G, CRUZ LA, COSTA FR, SILVA HP & FERREIRA JS. 2013. The largest flying reptile from Gondwana: a new specimen of *Tropeognathus* cf. *T. mesembrinus* Wellnhofer, 1987 (Pterodactyloidea, Anhangueridae) and other large pterosaurs from the Romualdo Formation, Lower Cretaceous, Brazil. An Acad Bras Cienc 85: 113-135. DOI 10.1590/S0001-37652013000100009.

KELLNER AWA & SARAIVA AF. 2019. Fósseis da Chapada do Araripe - uma odisseia no Cretáceo/ Fossils from the Chapada do Araripe - A Cretaceous Odyssey. Pró-Imagem Produções Fotográficas, 160p.

KELLNER AWA & TOMIDA Y. 2000. Description of a new species of Anhangueridae (Pterodactyloidea) with comments on the pterosaur fauna from the Santana Formation (Aptian-Albian), northeastern Brazil. Natl Sci Mus Monogr 17: ix-137.

KELLNER AWA, WANG X, TISCHLINGER H, DE ALMEIDA CAMPOS D, HONE DWE & MENG X. 2010. The soft tissue of *Jeholopterus* (Pterosauria, Anurognathidae, Batrachognathinae) and the structure of the pterosaur wing membrane. Proc R Soc B 277(1679): 321-329.

KUHN CES, CARVALHO IS, REIS FAGV, SPISILA AL & NOLASCO MC. 2022. Are Fossils Mineral or Cultural Heritage? The perspective of Brazilian Legislation. Geoheariтage 14:85 DOI 10.1007/s12371-022-00719-3.

LINDGREN J, CALDWELL MW, KONISHI T & CHIAPPE LM. 2010. Convergent evolution in aquatic tetrapods: insights from an exceptional fossil mosasaur. PLoS ONE 5(8): e11998.

MANZIG PC, KELLNER AWA, WEINSCHÜTZ LC, FRAGOSO CE, VEJA CS, GUIMARÃES GB, GODOY LC, LICCARDO A, RICETTI JH & DE MOURA CC. 2014. Discovery of a rare pterosaur bone bed in a Cretaceous desert with insights on ontogeny and behavior of flying reptiles. PloS ONE 9(8): e100005.

MARTILL DM & BECHLY G. 2007. Introduction to the Crato Formation. Camb Univ Press p. 3-7.

MARTILL DM, UNWIN DM, IBRAHIM N & LONGRICH N. 2018. A new edentulous pterosaur from the Cretaceous Kem Kem beds of south eastern Morocco. Cretac Res 84: 1-12.

MARTILL DM. 1994. Fake fossils from Brazil. Geol Today 10: 111-115.

PÊGAS RV, COSTA FR & KELLNER AWA. 2021. Reconstruction of the adductor chamber and predicted bite force in pterodactyloids (Pterosauria). Zool J Linn Soc 193(2): 602–635.

PÊGAS RV, LEAL MEC & KELLNER AWA. 2016. A Basal Tapejarine (Pterosauria; Pterodactyloidea; Tapejaridae) from the Crato Formation, Early Cretaceous of Brazil. PLoS ONE 11(9): e0162692.

PÊGAS RV, ZHOU X, JIN X, WANG K & MA W. 2023. A taxonomic revision of the *Sinopterus* complex (Pterosauria, Tapejaridae) from the Early Cretaceous Jehol Biota, with the new genus *Huaxiadraco*. PeerJ 11: e14829.

PINHEIRO FL ET AL. 2025. Cretaceous Pterosaurs of the Araripe Basin: A Comprehensive Taxonomic Update and Paleobiological Insights. An Acad Bras Cienc 97: e20250622. DOI 10.1590/0001-3765202520250622.

PINHEIRO FL, FORTIER DC, SCHULTZ CL, ANDRADE JFG & BANTIM RAM. 2011. New information on the pterosaur *Tupandactylus imperator*, with comments on the relationships of Tapejaridae. Acta Palaeontol Pol 56(3): 567-580.

SAYÃO JM & KELLNER AWA. 2006. Novo esqueleto parcial de pterossauro (Pterodactyloidea, Tapejaridae) do Membro Crato (Aptiano), Formação Santana, Bacia do Araripe, Nordeste do Brasil. Estud Geol 16: 16-40.

SCHNEIDER CA, RASBAND WS & ELICEIRI KW. 2012. NIH Image to ImageJ: 25 years of image analysis. Nat Methods 9: 671-675.

SELDEN PA, OLCOTT AN, DOWNEN MR, REN D, SHI CK & CHENG X. 2019. The supposed giant spider *Mongolarachne chaoyangensis*, from the Cretaceous Yixian Formation of China, is a crayfish. Palaeoentomology 002(5): 515-522.

SIMÕES TR, CALDWELL MW & KELLNER AWA. 2014. A new Early Cretaceous lizard species from Brazil, and the phylogenetic position of the oldest known South American squamates. J Syst Palaeontol 13(7): 601-614.

TISCHLINGER H & FREY E. 2002. Ein *Rhamphorhynchus* (Pterosauria, Reptilia) mitungewöhnlicher Flughauterhaltung aus dem Solnhofener Plattenkalk. Archaeopteryx 20: 1–20.

UNWIN DM & MARTILL DM. 2007. Pterosaurs of the Crato Formation. In: Martill DM, Bechly G & Loveridge RF (Eds),

The Crato Fossil Beds of Brazil—Window into an Ancient World, Cambridge: Cambridge University Press, p. 475-524.

VULLO R, MARUGÁN-LOBÓN J, KELLNER AWA, BUSCALIONI AD, GOMEZ B, FUENTE M & MORATALLA JJ. 2012. A new crested pterosaur from the early Cretaceous of Spain: the first European tapejarid (Pterodactyloidea: Azhdarchoidea). PLoS One 7(7): e83900.

WANG X & ZHOU Z. 2002. A new pterosaur (Pterodactyloidea, Tapejaridae) from the Early Cretaceous Jiufotang Formation of western Liaoning, China and its implications for biostratigraphy. Chin Sci Bull 47(20): 1521-1527.

WANG X ET AL. 2023. A new toothless pterosaur from the Early Cretaceous Jehol Biota with comments on the Chaoyangopteridae. Sci Rep 13(1): 22642.

WELLNHOFER P & BUFFETAUT E. 1999. Pterosaur remains from the Cretaceous of Morocco. Palaontol Z 73: 133-142

WELLNHOFER P & KELLNER AWA. 1991. The skull of *Tapejara wellnhoferi* Kellner (Reptilia, Pterosauria) from the Lower Cretaceous Santana Formation of the Araripe Basin, Northeastern Brazil. Am Mus Novit 3111: 1-19.

ZAMUDIO KR ET AL. 2018. Lack of science support fails Brazil. Science 361(6409): 1322-1323. DOI: 10.1126/science.aav3296.

ZHANG X, JIANG S, CHENG X & WANG X. 2019. New material of *Sinopterus* (Pterosauria, Tapejaridae) from the Early Cretaceous Jehol Biota of China. An Acad Bras Cienc 91: e20180756. https://doi.org/10.1590/0001-376520192018756.

ZHANG X, JIANG S, KELLNER AWA, CHENG X, COSTA FC & WANG X. 2023. A new species of *Eopteranodon* (Pterodactyloidea, Tapejaridae) from the Lower Cretaceous Yixian Formation of China. Cretac Res 149: 105573. DOI 10.1016/j.cretres.2023.105573.

How to cite

CANEJO L, SAYÃO JM & KELLNER AWA. 2025. Exploring the complex cranial morphology of *Tupandactylus imperator* (Pterodactyloidea, Tapejaridae) based on a new specimen. An Acad Bras Cienc 97: e20250756. DOI 10.1590/0001-3765202520250756.

Manuscript received on July 13, 2025;
accepted for publication on September 15, 2025

LUCAS CANEJO[1,2]
https://orcid.org/0000-0002-7974-8884

JULIANA M. SAYÃO[1,2]
https://orcid.org/0000-0002-3619-0323

ALEXANDER W.A. KELLNER[1,2]
https://orcid.org/0000-0001-7174-9447

[1]Universidade Federal do Rio de Janeiro, Museu Nacional, Laboratório de Sistemática e Tafonomia de Vertebrados Fósseis (LAPUG), Departamento de Geologia e Paleontologia, Campus de Ensino e Pesquisa, Av. Bartolomeu de Gusmão, 875, São Cristóvão, 20941-160 Rio de Janeiro, RJ, Brazil

[2]Universidade Federal do Rio de Janeiro, Museu Nacional, Programa de Pós-graduação em Zoologia (PPGZoo), Quinta da Boa Vista, s/n, São Cristóvão, 20940-040 Rio de Janeiro, RJ, Brazil

Correspondence to: **Lucas Canejo, Juliana Manso Sayão**
E-mails: canejo.francisco@gmail.com, jmsayao@mn.ufrj.br

Author contributions

LC: conceptualization, data curation, formal analysis, investigation, methodology, writing-original draft and figures editing; JMS: conceptualization, methodology, data curation, formal analysis, writing-review, editing, funding acquisition, and supervision; AWAK: conceptualization, funding acquisition, supervision, validation, writing-review, and editing.